Temporal shock wave analysis produced by copper exploding wires in air at atmospheric pressure

M. Barbaglia and G. Rodríguez Prieto

Articles you may be interested in

Study of the shock waves characteristics generated by underwater electrical wire explosion
J. Appl. Phys. **118**, 023301 (2015); 10.1063/1.4926374

Effects of load voltage on voltage breakdown modes of electrical exploding aluminum wires in air
Phys. Plasmas **22**, 062710 (2015); 10.1063/1.4923308

Peculiarity of convergence of shock wave generated by underwater electrical explosion of ring-shaped wire
Phys. Plasmas **20**, 052702 (2013); 10.1063/1.4804342

The techniques of metallic foil electrically exploding driving hypervelocity flyer to more than 10 km/s for shock wave physics experiments
Rev. Sci. Instrum. **82**, 095105 (2011); 10.1063/1.3633773

Characterization of converging shock waves generated by underwater electrical wire array explosion
Phys. Plasmas **15**, 112703 (2008); 10.1063/1.3023156

Temporal shock wave analysis produced by copper exploding wires in air at atmospheric pressure

M. Barbaglia[1,a)] and G. Rodríguez Prieto[2,b)]

[1]*Instituto de Física Arroyo Seco–IFAS (UNCPBA) and CIFICEN (UNCPBA-CICPBA-CONICET), Pinto 399, (7000) Tandil, Argentina*
[2]*Universidad de Castilla-la Mancha, I.N.E.I., Ciudad Real, Spain*

In this work, experimental results concerning the temporal evolution of the shock wave radii generated by an exploding copper wire of fixed length are presented. The variables of the experience were the diameter dimension—from 50 to 500 μm—and the initial capacitor voltage—from 5 to 25 kV. The diagnostic device was a streak shadow image system synchronized with the experiment. The result is a parametric collection of data showing the shock wave position across the time depicting the different stages of the experience. *Published by AIP Publishing.*
[http://dx.doi.org/10.1063/1.4966140]

I. INTRODUCTION

When a large enough electrical current passes through a metallic wire, the wire is heated through ohmic effect, converted into liquid, later vaporized, and finally transformed into plasma. The plasma free expansion generates a shock wave in the surrounding atmosphere. This phenomenon is called exploding wire (EW). This system was studied deeply because the matter appears in different states, and this is important for multiple purposes.[1–5] The edition work of Chace and Moore[6] and the work of Lebedev[7] constitute very good and extensive reviews of EW. From the beginning, electrical signals,[8–10] shock wave imaging,[11,12] and radiation measurement[13] were the primary tools to understand the phenomena. Because the shock wave generated has rich information about the shock wave generator system, different wire materials, dimensions, and surrounding media were studied in the past.[14–18] Here, we focus the study on a copper exploding wire at atmospheric pressure. The diameter of wire and charged voltage of the electrical system are used simultaneously as parameters in these experiments. The paper is structured as follows. After this Introduction, Section II describes the experimental setup employed, followed by a section with the results on the shock wave dynamics, and ending with some conclusions.

II. EXPERIMENTAL ARRANGEMENT

The experiments, objective of this work, were performed on the ALambre EXplosivo (ALEX) exploding wire system placed in the Institute for Energy Research and Industrial Applications (INEI), a research institute located in Ciudad Real (Spain) from Castilla-La Mancha University. The ALEX schematic is shown in Figure 1. The device constitutes a low inductance capacitor bank of 2.27 μF (two capacitors type Maxwell 33251) that is charged using a high voltage source. The discharge is controlled by a spark gap switch that is triggered by a high voltage pulse generator

(100 kV, 30 ns pulse width). The total measured fixed inductance of the system is 142 nH. The exploding wire is placed in open air with a fixed wire length of 3.3 cm, whereas the diameter is an independent variable; we used wires with the diameter of 50, 100, 250 and 500 μm. The distance between the wire and ground plane is 130 mm.

The measurements of the shock wave radii are obtained with a streak camera focused on the wire and illuminated by a continuous wave laser (532 nm/150 mW) passing by an arrangement of four lenses to expand the laser beam and
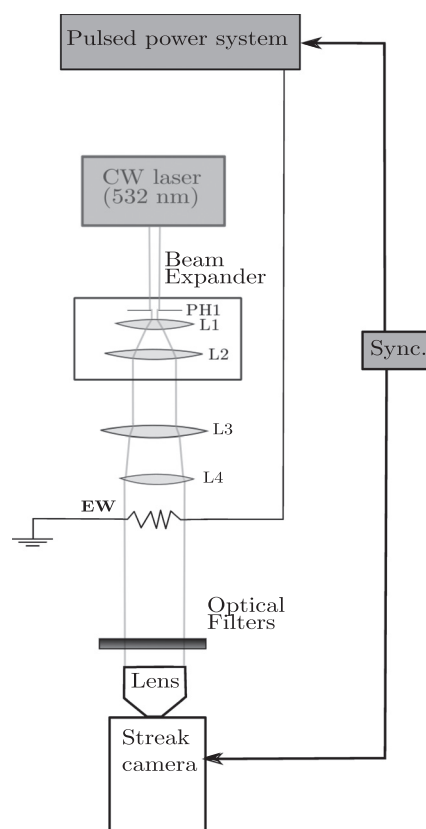

FIG. 1. ALEX experiment scheme. L1 to L4 are the lenses for the illumination system while that PH1 is a pinhole.

a)Electronic mail: mario.barbaglia@gmail.com
b)Electronic mail: gonzalo.rprieto@uclm.es

form a shadow imaging device. An interference filter centered in 532 nm allows only the laser light to pass through the lens system formed by a photographic objective, f 4.5 to 6.7, and two extension rings to be recorded by the streak camera. Images are stored in a computer, and after a temporal and space calibration for the each digital image, the shock wave dynamic evolution is accomplished. The streak camera system and the wire explosion are synchronized using the pulses of a standard delay pulse generator. Another independent variable is the capacitor voltage, varied between 5 and 25 kV, and it is used to observe and characterize the shock wave extension and plasma behavior generated in the metallic wire explosion in a broad range of energies.

III. RESULTS AND ANALYSIS

Typical shadowgraphs of copper wires with a diameter of 50 μm at various initial voltage charges are shown in Figure 2. Different plasma characteristics are visible on the features of the recorded light including the shock wave and the plasma channel.[16,17] We present here the measures of the exterior front radii as a function of time that include the expansion plasma and the shock wave stages. One of the most visible features is the reduction of the light absorption region at the beginning of the plasma expansion when the initial charging voltage increases its magnitude;[6] also, an increase in the rate of the radii of the shock wave is visible. Radial symmetry on the shock wave associated with a cylindrical expansion of the exploding wire[19] is not clearly visible
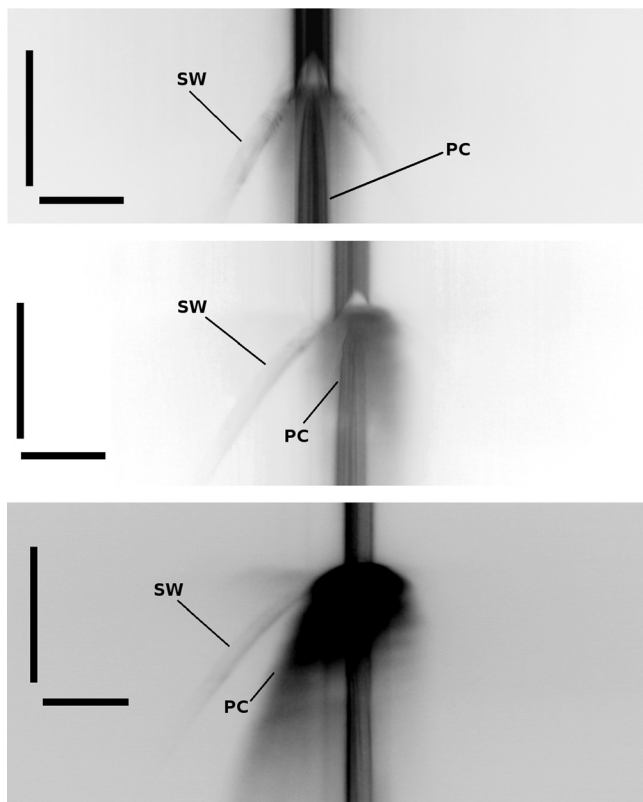
FIG. 2. From top to bottom; streak images of a copper wire with 50 μm diameter at 5 kV, 15 kV, and 25 kV. The horizontal and vertical mark represents 10 mm and 10 μs, respectively. In each image, the shock wave (SW) and the plasma channel (PC) are marked.

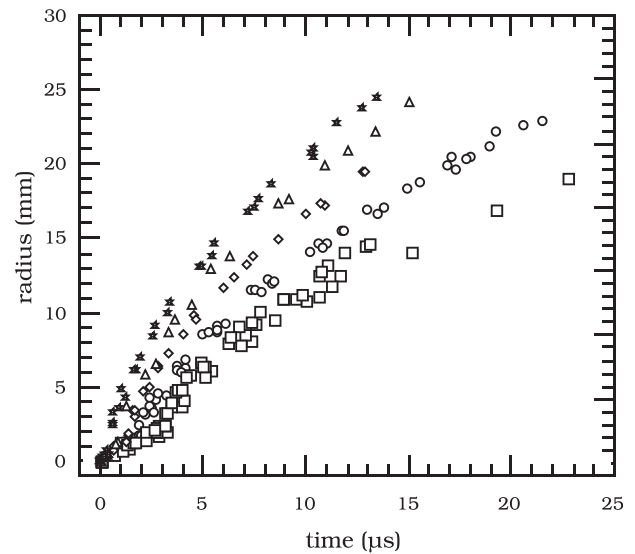FIG. 3. Shock wave radii as a time function of time at different voltages (50 μm diameter): □ 5 kV, ○ 10 kV, ◇ 15 kV, Δ 20 kV, and ☆ 25 kV.

in the shadowgraphs because of the uneven illumination produced by the laser-lens system used in these experiments, despite the careful alignment of the setup. Examination of the raw images shows that both sides of the shock wave are symmetrically expanding; therefore, in order to obtain the radial expansion, the more visible side was employed.

Figures 3, 5, 6, and 8 show the shock wave radii position over time, produced by a copper exploding wire of diameters 50, 100, 250, and 500 μm, respectively. These radii of the shock waves, at the end of the recorded image, are always approximated by straight lines of different slopes; therefore, the final rate of radii can be considered as constant. The magnitude of the slope becomes larger with the increase in the initial charging voltage regardless of the wire diameter. As a consequence, it follows that the final rate of radii increases with the magnitude of the initial charging voltage.
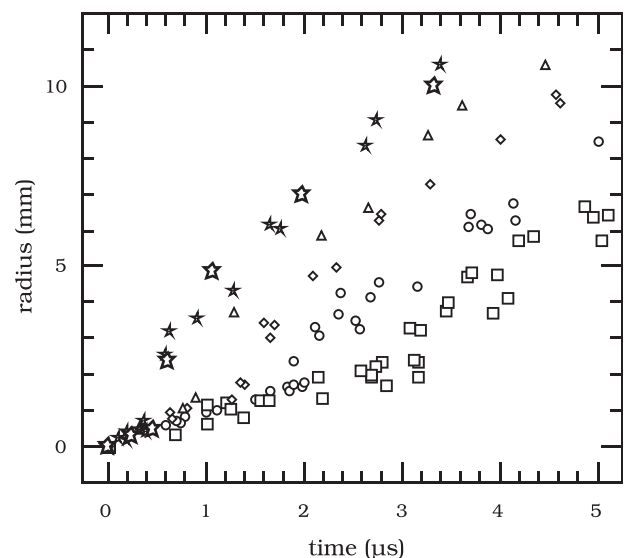
FIG. 4. Shock wave radii as a function of time, at the earliest stages, at different voltages (50 μm diameter): □ 5 kV, ○ 10 kV, ◇ 15 kV, Δ 20 kV, and ☆ 25 kV.
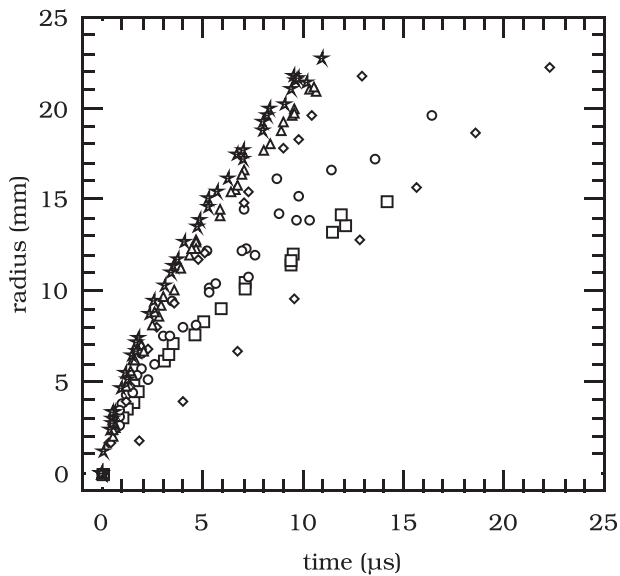
FIG. 5. Shock wave radii as a function of time at different voltages (100 μm diameter): □ 5 kV, ○ 10 kV, ◇ 15 kV, Δ 20 kV, and ☆ 25 kV.

FIG. 6. Shock wave radii as a function of time at different voltages (250 μm diameter): ◆ 5 kV, ■ 6 kV, ● 7 kV, ▶ 8 kV, □ 10 kV, ○ 12 kV, Δ 15 kV, * 18 kV, × 20 kV, and ☆ 25 kV.

Figures 3 and 4 show the data collected for a wire of 50 μm diameter. Three stages can be distinguished in Figure 3: an increase in the initial low rate of the radii is followed by an acceleration stage, and finally, a deceleration stage leading smoothly to a final rate of the radii that are roughly constant. The general tendency of a faster shock wave rate of the radii increases for larger charging voltages and is also present at the 50 μm diameter wires, as it can be illustrated by the values of the radius at 5 μs after the beginning of the phenomena. When the charging voltage is increased from 5 to 25 kV, the radius at 5 μs changes from 6 to 14 mm, a difference of a factor of two between both values. At this diameter, the first stage of radial front of copper wires is very similar for all the charging voltages, as shown in Fig. 4. It is also visible in this figure that more time is required to increase the radii as the charging voltages are reduced.

Radii of shock waves from copper wires with the diameter of 100 μm are presented in Figure 5 (in contrast with the previous case, only the last two stages are visible: the accelerated stage and the final one, roughly constant, the rate of the radii increases due to the shortening of the deceleration stage). As for the 50 μm diameter wires, the first accelerated stage is very similar for all the charging voltages, as it is shown in the figure. On the other hand, the final stage shows a clear dependence on the initial charging voltage indicated by a notorious change in the shock wave final radius. Using the radial value at 5 μs after the beginning of the explosion, a variation from 8 to 15 mm is observed when the charging voltage is increased from 5 to 25 kV.

For the diameter of 250 μm, an expanded set of initial energy was used. This increment has been made to explore in more detail about the dependence of the radii of the shock wave with the energy. Two distinct behaviors can be deduced using all the radial data values from Figure 6. A single stage expansion is observed with just an increase in the constan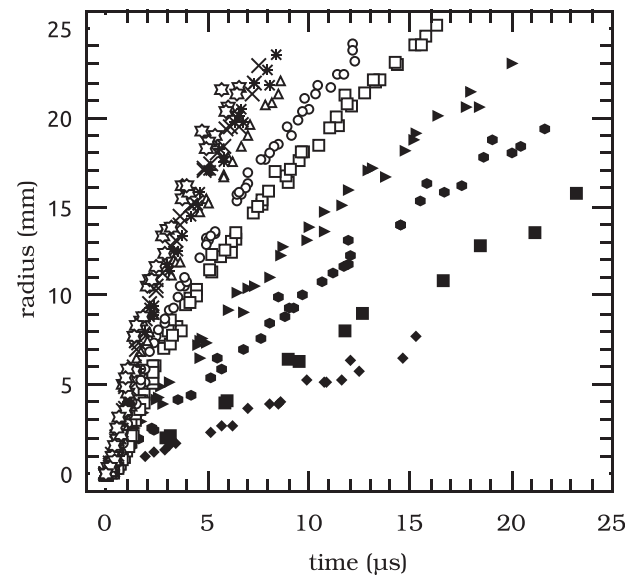t rate of the radii. Therefore, a straight line trajectory is visible for the lowest charging voltages as Figure 7 shows. With the use of a linear approximation for the shock wave radius, a change in the slope from 0.478 ± 0.001 to 0.94 ± 0.01 mm/μs is visible, whereas the charging voltage increases from 5 to 7 kV. When the capacitors were charged above 8 kV, it can be seen a radial increase in the shock wave in two phases, which are found in similar behavior to 100 μm diameter wires. Furthermore, at the beginning of the explosion, the acceleration of the shock wave is faster than the final acceleration. Radii of the shock wave at 5 μs are markedly different. For an initial charging voltage of 5 kV, the radius is 2 mm and it reaches the 19 mm for the maximum charging voltage of 25 kV. In this case, a difference in radius of 17 mm is achieved meaning a large deviation from the values measured in previous experiments.
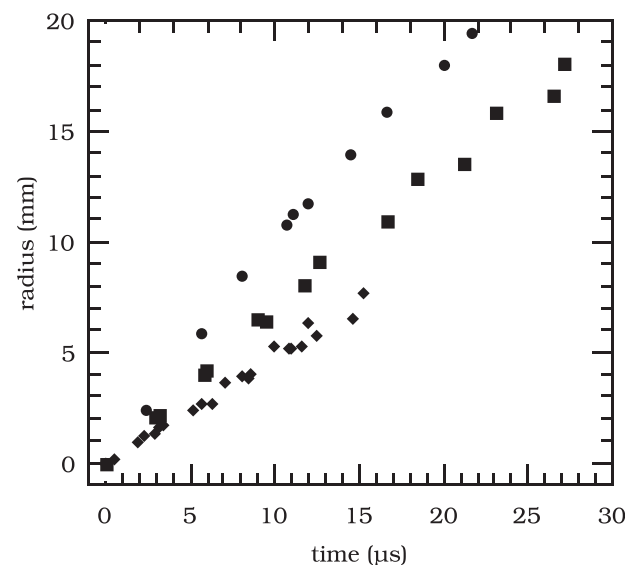

FIG. 7. Shock wave radii as a function of time at different voltages (250 μm diameter): ◆ 5 kV, ■ 6 kV, and □ 7 kV.
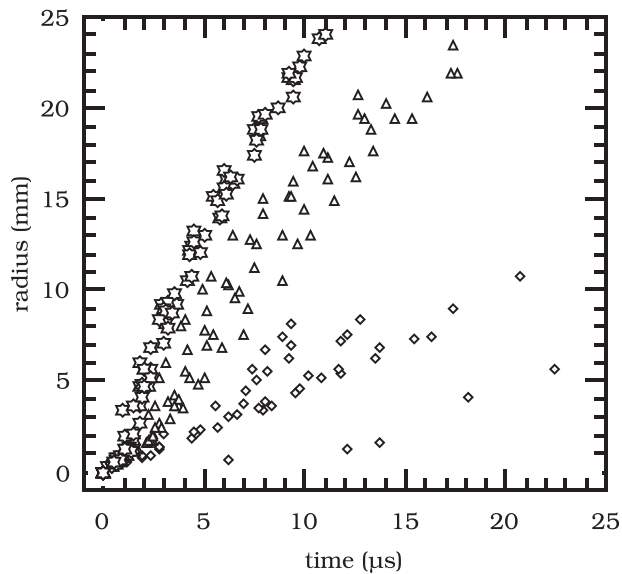
FIG. 8. Shock wave radii as a function of time at different voltages (500 μm diameter): ◇ 15 kV, △ 20 kV, and ☆ 25 kV.

TABLE I. Calculated mean shock wave rates of the radii at 5 μs.

Wire diameter (μm)	Voltage (kV)	Rate of the radii raise (mm/μs)
50	5	1.0
50	10	1.1
50	15	1.2
50	20	1.3
50	25	1.4
100	5	0.7
100	10	1.1
100	15	1.3
100	20	1.4
100	25	1.5
250	5	0.4
250	6	0.8
250	7	1.0
250	8	1.1
250	10	1.4
250	12	1.5
250	15	1.8
250	18	2.0
250	20	2.1
250	25	2.2
500	15	0.4
500	20	1.5
500	25	1.9

Due to the high data point dispersion, the observation of the dynamic of the shock wave, when a wire of 500 μm diameter is used, is more complicated, as it is seen in Figure 8. In fact, when the minimum initial energy is used, the data dispersion causes only the general trend of increase in the final constant rate of the radii to be visible. For the radial value above 5 μs, a value of 2 mm is observed when the capacitors are charged to 15 kV whereas it reaches 13 mm when the capacitors are charged to 25 kV. The difference between these two radii, 11 mm, is then larger than for wires of 50 and 100 μm diameters and in the same order of magnitude than the value for the wires of 250 μm diameter.

From the Figures, it can be appreciated larger values for the shock wave radius when the initial charging voltage increases, as shown in Figures 3 to 8. In Figure 8, the measured final radii of the shock waves change from a value on the order of 5 mm at 15 kV to a value of approximately 25 mm at the maximum charging voltage.

With the results obtained from this experiment, a mean rate of the radii raise of the shock wave by means of the radii curves can be estimated. The values calculated at 5 μs are shown in Table I. For a wire diameter of 50 μm, the observed change on slopes obtained—from Figure 3—increases from 1 to 1.4 mm/μs when the initial voltage charge is increased from 5 to 25 kV, respectively. The same behavior is observed with the wire diameters of 100 and 250 μm, as shown in Figures 5 and 6. Thus, in the former case of the 100 μm wire, estimations of the final shock wave rate of the radii raise for a voltage charge of 5 and 25 kV go from 0.7 to 1.5 mm/μs, respectively. On the other hand, the rate of the radii raise varies from 0.4 to 2.2 mm/μs with the wire diameter of 250 μm on the same voltages. For wire diameter of 500 μm, the rate of the radii raise varies from 0.4 to 1.9 mm/μs when the voltage is between 15 kV and 25 kV.

A rude comparison with the experiment of Grinenko *et al.* shows that, for similar wire section, they obtain a shock wave velocity greater than those obtained here. Because the medium used was water and the initial energy used here is minor, to be precise in the comparison, a special attention should be put to the manner in which the energy is delivered to the wire (what is out of the scope of this work). The observed decay rates of the radii with the time in Figures 3, 5, and 6 are related to the fact that the energy available for the shock wave must be distributed in larger radius across the time (geometric decay). Because of this, a slow down on the rates of the radii at the final stage is measured.[14]

IV. CONCLUSIONS

We have studied the radial position of the shock wave produced by a copper explosive wire surrounded by air at atmospheric pressure in a broad range of energies and masses, the latter through the use of different wire diameters. The energy provided to the wire by the capacitors bank modifies the radial position of the shock wave, as it is observed in this work. A detailed record of the transition between them is shown for the 250 μm diameter wire by means of an expanded values set of initial energies on the system.

From the measured shock wave radii, estimations on the mean rate of the radii raise value were obtained in this work. Also, it was observed that for all the diameters studied, an increase in the maximum radial expansion when the initial capacitors voltage was increased. Such tendency is related with the increase of energy delivered to the metallic wire.[14]

[1] I. I. Beilis, A. Shashurin, R. B. Baksht, and V. Oreshkin, J. Appl. Phys. **105**, 33301 (2009).

[2] G. S. Sarkisov, P. V. Sasorov, K. W. Struve, and D. H. McDaniel, J. Appl. Phys. **96**, 1674 (2004).

[3] P. Sen, J. Ghosh, A. Abdullah, P. Kumar, and Vandana, J. Chem. Sci. **115**, 499 (2003).

[4] A. Vanderburg, F. Stefani, A. Sitzman, M. Crawford, D. Surls, C. Ling, and J. McDonald, IEEE Trans. Plasma Sci. **42**, 3167 (2014).

[5] D. A. Hammer and D. B. Sinars, Laser Part. Beams **19**, 377 (2001).

[6] *Exploding Wires*, edited by, W. G. Chace and H. K. Moore (Springer, Boston, MA, USA, 1968).

[7] S. V. Lebedev and A. I. Savvatimskiĭ, Sov. Phys. Usp. **27**, 749 (1984).

[8] G. S. Sarkisov, S. E. Rosenthal, and K. W. Struve, Rev. Sci. Instrum. **78**, 43505 (2007).

[9] G. R. Prieto, L. Bilbao, and M. Milanese, Laser Part. Beams **34**, 263 (2016).

[10] L. Bibbo, N. Giovambatista, P. Gomez, M. Olivieri, C. Tibaldi, L. Bernal, J. Pouzo, and L. Bilbao, Astrophys. Space Sci. **256**, 467 (1997).

[11] G. L. Clark, J. J. Hickey, R. J. Kingsley, and R. F. Wuerker, in *Exploding Wires* (Springer, 1962), pp. 175–180.

[12] A. Grinenko, A. Sayapin, V. T. Gurovich, S. Efimov, J. Felsteiner, and Y. E. Krasik, J. Appl. Phys. **97**, 23303 (2005).

[13] D. J. Strickland and D. L. Lin, IEEE Trans. Nucl. Sci. **25**, 1571 (1978).

[14] I. I. Beilis, R. B. Baksht, V. I. Oreshkin, A. G. Russkikh, S. A. Chaikovskii, A. Y. Labetskii, N. A. Ratakhin, and A. V. Shishlov, Phys. Plasmas **15**, 013501 (2008).

[15] A. G. Rousskikh, V. I. Oreshkin, A. Zhigalin, I. I. Beilis, and R. B. Baksht, Phys. Plasmas **17**, 033505 (2010).

[16] F. A. Grinenko, Ya. E. Krasik, S. Efimov, A. Fedotov, V. Tz. Gurovich, and V. I. Oreshkin, Phys. Plasmas **13**, 042701 (2006).

[17] S. I. Tkachenko, D. V. Barishpoltsev, G. V. Ivanenkov, V. M. Romanova, A. E. Ter-Oganesyan, A. R. Mingaleev, T. A. Shelkovenko, and S. A. Pikuz, Phys. Plasmas **14**, 123502 (2007).

[18] S. Sahoo, A. K. Saxena, T. C. Kaushik, and S. C. Gupta, High Energy Density Phys. **17B**, 270–276 (2015).

[19] F. D. Bennett, R. Hefferlin, and R. A. Strehlow, in *Progress in High Temperature Physics and Chemistry*, edited by C. A. Rouse (Pergamon Press, 1969), Vol. 2.